Radiation Measurements 44 (2009) 344–350

Contents lists available at ScienceDirect

Radiation Measurements

journal homepage: www.elsevier.com/locate/radmeas

A new look at the linear-modulated optically stimulated luminescence (LM-OSL) as a tool for dating and dosimetry

Reuven Chen [a,*], Vasilis Pagonis [b], John L. Lawless [c]

[a] Raymond and Beverly Sackler School of Physics and Astronomy, Tel-Aviv University, Tel-Aviv 69978, Israel
[b] Physics Department, McDaniel College, Westminster, MD 21157, USA
[c] Redwood Scientific Incorporated, Pacifica, CA 94044-4300, USA

ARTICLE INFO

Article history:
Received 24 August 2008
Received in revised form
3 March 2009
Accepted 15 March 2009

Keywords:
LM-OSL
Dose dependence
Dosimetry
Dating
OTOR model

ABSTRACT

Optically stimulated luminescence (OSL) has been in use for dosimetry and dating in the last two decades. Since the OSL dependence on time is a featureless decaying function, a linear-modulation of the stimulating-light intensity has been suggested [Bulur, E., 1996. An alternative technique for optically stimulated luminescence. Radiat. Meas. 26, 701–709.], which resulted in a peak-shaped curve. The properties of this curve have been studied, assuming first-, second- and general-order kinetics. In a recent paper we have shown [Chen, R., Pagonis, V., 2008. A unified presentation of thermoluminescence (TL), phosphorescence and linear-modulated OSL (LM-OSL). J. Phys. D: Appl. Phys. 41, 035102 (1–6).] that for general-order curves, the peak maximum cannot be expected to depend linearly on the dose of excitation. A new presentation of the LM-OSL has been suggested, in which the peak maximum is linear with the filling of trapping states, which, in turn, may be expected to be linear with the dose under appropriate conditions. In the present work, we report on results of numerical simulation of the LM-OSL using the one trap-one recombination center (OTOR) model, dealing with the traffic of carriers between one trapping state, one kind of recombination center and the conduction and valence bands during excitation and read-out, and without making any simplifying assumptions. The process during optical read-out has been followed in the simulation that consisted of the numerical solution of the relevant sets of coupled differential equations, and also by analytical treatment. Sets of parameters leading to approximately first- and second-order kinetics, and to intermediate cases, have been used and the results presented in the original and the new ways are shown. The consequences concerning dating and dosimetry are discussed.

1. Introduction

Optically stimulated luminescence (OSL) has been recognized as an important tool for dosimetry and for archaeological and geological dating (see e.g. Huntley et al., 1985). Bulur (1996) suggested changing the featureless OSL decay curve into a peak-shaped function by increasing the intensity of the stimulating-light linearly with time. For the linear-modulated OSL (LM-OSL) and first-order kinetics, the governing equation is

$$L(t) = -\mathrm{d}n/\mathrm{d}t = (I_0\alpha/\theta)tn(t), \tag{1}$$

where $L(t)$ is the emitted light intensity and t is the time, and where θ (s) is the duration of the observation and αI_0 (s^{-1}) is the probability of escape of electrons from the traps at a light intensity of stimulation I_0. The stimulating-light intensity here varies with time as I_0t/θ. The solution of this equation yields the intensity measured under these circumstances as a function of time

$$L(t) = (\alpha t/\theta)n_0 I_0 \exp\left[-(\alpha I_0/2\theta)t^2\right], \tag{2}$$

where n_0 is the initial occupancy of traps following excitation. This equation represents a peak-shaped function. As shown by Bulur (1996), the maximum intensity here is given by

$$L_{\max} = n_0(\alpha I_0/\theta)^{1/2}\exp(-1/2), \tag{3}$$

which is very useful in dosimetry applications since the maximum intensity is proportional to the initial concentration of trapped carriers n_0. This, in turn, is assumed to carry the information which concerns the absorbed dose. It is quite obvious that integration of Eq. (2) from 0 to infinity yields n_0. Thus, if one takes as the LM-OSL signal either the maximum intensity or the whole area under the

* Corresponding author. Tel.: +972 3 640 8426; fax: +972 9 95 61213.
E-mail address: chenr@tau.ac.il (R. Chen).

1350-4487/$ – see front matter © 2009 Elsevier Ltd. All rights reserved.
doi:10.1016/j.radmeas.2009.03.019

curve, in the first-order case, the signal is proportional to the concentration following the excitation, n_0.

Bulur (1996) gave a similar treatment to LM-OSL governed by general-order kinetics. The governing equation here is

$$L(t) = -\mathrm{d}n/\mathrm{d}t = (\gamma I_0/\theta)tn^b, \tag{4}$$

where γ is a constant. Bulur (1996) assumed that $\gamma = \alpha/n_0^{b-1}$, where α is the frequency factor. Bulur and Göksu (1999) changed this assumption to $\gamma = \alpha/N^{b-1}$ where N is the concentration of trapping states, a similar assumption to that given by Rasheedy (1993) for general-order TL. Using the latter definition, the solution of Eq. (4) is

$$L(t) = n_0^b(\alpha I_0)\left[t/\left(N^{b-1}\theta\right)\right] \times \left\{1+(b-1)\left[\alpha I_0 n_0^{b-1}/\left(2\theta N^{b-1}\right) \times\right]t^2\right\}^{-b/(b-1)}. \tag{5}$$

Note that the general-order equation is merely an empirical presentation of cases intermediate in some sense between first and second order. An important special case is that of second-order kinetics, first suggested by Garlick and Gibson (1948), which takes place in cases of either dominating retrapping or of equal recombination and retrapping-probability coefficients (see e.g. P. 31 in Chen and McKeever, 1997). Here, we have for Eqs. (4) and (5) $b = 2$ and obtain

$$L(t) = \frac{n_0^2[\alpha I_0/(N\theta)]t}{\left\{1+[\alpha I_0 n_0/(2N\theta)]t^2\right\}^2}. \tag{6}$$

By equating the derivative of Eq. (5) to zero, one obtains

$$t_{\max} = \sqrt{\frac{2}{(b+1)}\frac{\theta}{\alpha I_0}\left(\frac{N}{n_0}\right)^{b-1}}. \tag{7}$$

By inserting Eq. (7) into (5) one obtains

$$L_{\max} = 2\left[\frac{\alpha I_0(b+1)}{\theta N^{b-1}}\right]^{1/2}\left(\frac{2b}{b+1}\right)^{-b/(b-1)} n_0^{(b+1)/2}. \tag{8}$$

In a recent work, Chen and Pagonis (2008) have suggested a new presentation of LM-OSL results. Instead of the conventional way of plotting the LM-OSL intensity as a function of time, they suggested to plot $y = t\cdot L(t)$ vs. $x = 2\ln t$ ($t^2 = e^x$). One should be cautious about the dimensions of t and x. As defined, t has, obviously, units of s, and its logarithm cannot be defined. In order to have a dimensionless time, we can define $t_0 = 1$ s and consider $t' = t/t_0$, which is dimensionless, but has the same numerical value as t. This solves also the problem of writing $t^2 = e^x$, where the left-hand side is dimensional and the right-hand side dimensionless; with t' as defined here, the problem is solved. Keeping this in mind, we'll continue using t while meaning the dimensionless t'.

Making this transformation yields for first order

$$y(x) = 2n_0\delta e^x \exp(\delta e^x), \tag{9}$$

where $\delta = \alpha I_0/(2\theta)$. The maximum intensity of this curve is given by

$$y_m = 2n_0/e. \tag{10}$$

As shown by Chen and Pagonis (2008), the expression for general order in the new variables is

$$y(x) = 2n_0\delta' e^x\left[1+(b-1)\delta' e^x\right]^{-b/(b-1)}. \tag{11}$$

where $\delta' = \alpha I_0 n_0/(2\theta N)$. The maximum intensity for general order is given by

$$y_m = \frac{2n_0}{b^{b/(b-1)}}, \tag{12}$$

Thus, in the new presentation, when first-order or general-order kinetics, including the second-order case, governs the process, y_m, the maximum of the $y(x)$ curve must be linear with the initial concentration of carriers (following excitation by radiation). Note that this presentation is rather similar to the way of transforming the phosphorescence decay graph into a peak-shaped curve suggested first by Randall and Wilkins (1945) and elaborated upon by Visocekas (1978) and Chen and Kristianpoller (1986). Chen and Pagonis (2008) showed that in the conventional presentation, the maximum intensity of the emitted signal can be expected to be superlinear with the initial concentration of trapped carriers, n_0, for general-order kinetics. From Eq. (8), we immediately see that $L_{\max} \propto n_0^{(b+1)/2}$, which yields linear dependence on n_0 for first order, as pointed out above, and an $n_0^{3/2}$ dependence for second order. They have also shown that the area under the $y(x)$ curve is $\int_{-\infty}^{\infty} y(x)\mathrm{d}x = 2n_0$, namely, proportional to n_0. In cases where n_o is proportional to the dose, similar dependencies on the dose can be expected for the conventional and new presentations.

In the present work, we simulate the LM-OSL curves, using the relevant differential rate equations, during the read-out stage of the optical stimulation, and assuming the simplest possible one trap-one recombination-center model. We do this for sets of parameters leading to first-order, second-order and to intermediate situations. We also use the quasi-steady assumption to develop an analytical solution. The results are shown in the original and the above mentioned new presentation, and conclusions are drawn concerning the dependence on the initial concentration n_0.

2. The model

The model shown in Fig. 1 is the simplest possible one trap-one recombination center (OTOR) for explaining the optically stimulated luminescence, including, of course, the LM-OSL. The meaning of the different magnitudes is given in the caption. The equations governing the process during the optical stimulation are

$$L(t) = -\frac{\mathrm{d}m}{\mathrm{d}t} = A_m m n_c, \tag{13}$$

$$\frac{\mathrm{d}n}{\mathrm{d}t} = A_n(N-n)n_c - fn, \tag{14}$$

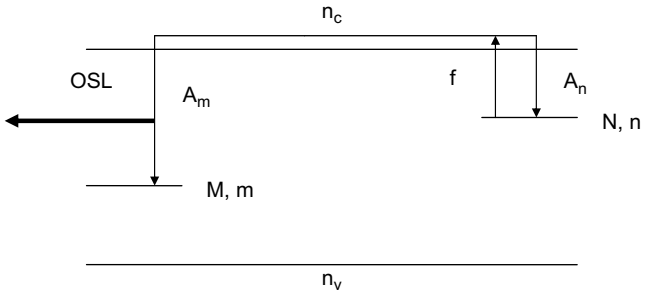

Fig. 1. Energy level diagram of the OTOR model. N (cm^{-3}) and M (cm^{-3}) are the concentrations of electron trapping state and hole recombination centers; n (cm^{-3}) and m (cm^{-3}) are their instantaneous occupancies, respectively. f (s^{-1}) is the optical stimulation rate, such that the rate per cm^3 per second is $f\cdot n$. Here, $f = f_0\cdot t$ where $f_0(\mathrm{s}^{-2})$ is constant. The instantaneous concentration of free electrons in the conduction band is n_c (cm^{-3}) and A_m, A_n are the recombination-probability and retrapping-probability coefficients, respectively.

$$\frac{dn_c}{dt} = \frac{dm}{dt} - \frac{dn}{dt}, \tag{15}$$

where $f(s^{-1})$ is proportional to the stimulating-light intensity. The linear modulation is achieved by increasing f linearly with time during read-out, namely, $f = f_0 \cdot t$, where f_0 (s^{-2}) is constant. Due to the very simple model, at the end of irradiation and relaxation, one can expect an equal number of electrons and holes to be trapped in trapping states and recombination centers, respectively. In the present work we, therefore, skip the first steps of excitation and relaxation, assume values of n_0, and solve the equations for the read-out stage for different values of n_0. The dependence of the maximum LM-OSL curve on n_0 will be monitored for different sets of parameters, both in the original and new presentations. The possible dependencies of n_0 on the excitation dose within the OTOR model are discussed elsewhere (Lawless et al., in press).

A short discussion on the choice of sets of parameters is given here. As pointed out above, we would like to follow cases that are close to first order, second order and intermediate cases. In all these cases, we can make the quasi-steady assumption, namely that n_c is significantly smaller than n and m, and $|\frac{dn_c}{dt}| << |\frac{dn}{dt}|; |\frac{dm}{dt}|$. To begin with, obviously the properties of the solution depend on the relation between A_n and A_m, however for the quasi-equilibrium to hold, both probability coefficients are to be large enough so that the values of n_c are significantly smaller than those of m. Halperin and Braner (1960), gave an approximate equation for TL when quasi-equilibrium holds. The direct analogy for the present case of OSL is

$$L = -\frac{dm}{dt} = fn\frac{A_m m}{A_m m + A_n(N-n)}. \tag{16}$$

As pointed out above, in the OTOR, and when quasi-equilibrium holds, $n = m$. When $A_m m \gg A_n(N-n)$, the first-order equation results immediately, namely

$$L = -\frac{dn}{dt} = f \cdot n. \tag{17}$$

Note that $A_m \gg A_n$ is not a sufficient condition for Eq. (17) to be a good approximation since $N-n$ may be significantly larger than m. The functional condition $A_m m \gg A_n(N-n)$ must hold for the first-order kinetics to take place. Moreover, since m and n decrease along the LM-OSL measurement, one may start with $A_m m$ being much larger than $A_n(N-n)$, but the relation between them may change along the measurement. Thus, an LM-OSL peak may start as being of first order, and later continue as having non-first-order kinetics. Note also that since, as pointed out above, $f = f_0 t$, Eq. (17) is the same as Eq. (1) where $f_0 = \alpha I_0/\theta$.

The second-order kinetics can result from Eq. (14) in one of two ways. If $A_m = A_n$ (and since with this simple model $m = n$), we get

$$L(t) = -\frac{dn}{dt} = \frac{f_0}{N} t n^2. \tag{18}$$

The condition that the two probability coefficients be equal is not very likely to take place since the trapping state and recombination center are two independent entities, associated with two different impurities or defects in the sample. Another way to get the second-order kinetics is assuming that retrapping dominates, $A_n(N-n) \gg A_m m$, and that the trap is far from saturation, $N \gg n$. Like in the first-order case, these are assumed relations between variables rather than parameters. However, since m and n decrease during the measurement, if the conditions hold at the beginning, they remain so all along the measurement, and therefore, if a peak starts being of second order it remains being of second order all along. The governing equation here is

$$L(t) = -\frac{dn}{dt} = \frac{f_0 A_m}{N A_n} t n^2 \tag{19}$$

It appears more likely to get second-order kinetics with the dominating retrapping condition than with the equal probability coefficients. In any case, both Eqs. (18) and (19) are the same (with substitution of the relevant constants, $\gamma I_0/\theta = f_0 A_m/N A_n$) as Eq. (4) with $b = 2$, and therefore Eq. (6) is its solution. Note that there are many intermediate cases in which $A_m m$ is of the same order as $A_n(N-n)$. These cannot be precisely presented by the "general-order" equation.

3. Theory

In Section 4, we present numerical solutions of Eqs. (13–15) for sample sets of the five parameters: A_m, A_n, f_0, n_0 and N. In this section, we use the quasi-steady assumption to develop an analytical solution. Then, we develop scaling laws that reduce the number of parameters that must be studied. The value of this reduction will be shown in the plots presented in Section 4. Starting with Eq. (16) of the OTOR model, and substituting $n = m$ and $f = f_0 t$ we find

$$L = -\frac{dn}{dt} = f_0 t \frac{A_m n^2}{A_m n + A_n(N-n)}, \tag{20}$$

which is subjected to the initial condition of $n = n_0$ at $t = 0$. This can be immediately integrated

$$\frac{A_m - A_n}{A_n}\ln\left(\frac{n_0}{n}\right) + \frac{A_n N}{A_m}\left(\frac{1}{n} - \frac{1}{n_0}\right) = \frac{1}{2} f_0 t^2. \tag{21}$$

Equation (21) can be rearranged to solve for t as a function of n,

$$t = \sqrt{\frac{2}{f_0}\left[\frac{A_m - A_n}{A_m}\ln\left(\frac{n_0}{n}\right) + \frac{A_n N}{A_m}\left(\frac{1}{n} - \frac{1}{n_0}\right)\right]}. \tag{22}$$

Combining Eqs. (20) and (22), the luminescence L can be found as a function of n alone,

$$L = \sqrt{2 f_0\left[\frac{A_m - A_n}{A_m}\ln\left(\frac{n_0}{n}\right) + \frac{A_n N}{A_m}\left(\frac{1}{n} - \frac{1}{n_0}\right)\right]}\frac{A_m n^2}{A_m n + A_n(N-n)}. \tag{23}$$

We are also interested in the transformed luminescence, tL, which is found from Eqs. (22) and (23),

$$y = tL = 2\left[\frac{A_m - A_n}{A_m}\ln\left(\frac{n_0}{n}\right) + \frac{A_n N}{A_m}\left(\frac{1}{n} - \frac{1}{n_0}\right)\right]\frac{A_m n^2}{A_m n + A_n(N-n)}. \tag{24}$$

Now, we have t, L and tL, all as explicit functions of n in Eqs. (22–24). In order to create plots of L as a function of t and of Lt as a function of $2\ln t$, we choose a series of n in the range $0 \le n \le n_0$. For each such value of n, we can use Eqs. (22) and (23) to compute the values of time t and luminescence L which occur when the density reaches n. This provides a point for use on a plot of L vs. t. Similarly, by choosing various values of n, we can create the transformed plot of tL vs. $2\ln t$.

We can simplify Eqs. (22–24) by defining the following non-dimensional quantities

$$\hat{t} = t\sqrt{f_0}, \tag{25}$$

$$\hat{n} = n/N, \tag{26}$$

$$\hat{L} = \frac{L}{N\sqrt{f_0}}, \tag{27}$$

$$\widehat{A} = A_n/A_m. \tag{28}$$

Using these variables, Eqs. (22–24) can be rewritten as

$$\widehat{t} = \sqrt{2\left[\left(1-\widehat{A}\right)\ln\left(\frac{\widehat{n_0}}{\widehat{n}}\right)+\widehat{A}\left(\frac{1}{\widehat{n}}-\frac{1}{\widehat{n_0}}\right)\right]}, \tag{29}$$

$$\widehat{L} = \sqrt{2\left[\left(1-\widehat{A}\right)\ln\left(\frac{\widehat{n_0}}{\widehat{n}}\right)+\widehat{A}\left(\frac{1}{\widehat{n}}-\frac{1}{\widehat{n_0}}\right)\right]}\frac{\widehat{n}^2}{\widehat{n}+\widehat{A}\left(1-\widehat{n}\right)}, \tag{30}$$

$$\widehat{t}\widehat{L} = 2\left[\left(1-\widehat{A}\right)\ln\left(\frac{\widehat{n_0}}{\widehat{n}}\right)+\widehat{A}\left(\frac{1}{\widehat{n}}-\frac{1}{\widehat{n_0}}\right)\right]\frac{\widehat{n}^2}{\widehat{n}+\widehat{A}\left(1-\widehat{n}\right)}. \tag{31}$$

Whereas the right-hand sides of Eqs. (22–24) depend on six quantities, A_m, A_n, f_0, N, n_0 and n, in Eqs. (29–31), the right-hand sides depend on only three quantities, $\widehat{n}$, $\widehat{n_0}$ and $\widehat{A}$. The use of these new equations is discussed below.

4. Numerical results

In order to check the dependence on the initial concentration, n_0, of the original as well as the revised LM-OSL curves, we chose sets of parameters, and solved numerically Eqs. (13–15) for different values of the initial traps and centers occupancy, $n_0 = m_0$, using the Matlab ode23s solver. Alternatively, we used Eqs. (29–31) and proceeded as explained below. The figures shown below are of the simulation, but the results of both methods were exactly the same. The exact agreement of the two approaches is related to the choice of parameters such that the quasi-steady assumption for free carriers prevails. We then changed the value of the initial occupancies, and observed the variations in the peak shape. This has been done for cases of first order, second order of the two types mentioned above and for intermediate cases. Throughout the simulation process, we monitored the values of $A_m m$ and $A_n(N-n)$, and compared them in order to see whether the conditions mentioned above are fulfilled. We have also monitored the values of n_c and n in order to verify that the quasi-steady condition holds.

Fig. 2 shows the results of the simulation for the set of parameters given in the caption. Here, A_m is 5 orders of magnitude larger than A_n, and first-order kinetics can be expected. Indeed, mA_m is found to be 3–4 orders of magnitude larger than $A_n(N-n)$ in the simulations. The result is a peak in the LM-OSL curve, which does not shift with the change of the initial value of n_0. As seen in the graph, the maximum intensity doubles from one curve to the next, as expected when n_0 varies by factors of 2. Fig. 3 shows the same results in the new way suggested by Chen and Pagonis (2008). The peaks here are very similar in shape to first-order TL peaks. As expected, the maxima are linearly dependent on n_0.

Fig. 4 shows the results of simulations with the parameters given in the caption. Here, A_n is larger than A_m, and along with N being significantly larger than m, $A_n(N-n) \gg A_m m$, and the second-order kinetics results. Like in TL, the peak shifts to lower values of t for higher values of n_0. As for the maximum intensity, it is readily seen to increase superlinearly with n_0. For example, while going from curve (a) to (e), n_0 increases by a factor of 16, and L_{max} by $\sim$64, which, indeed is $16^{3/2}$. Fig. 5 shows the same results in the new presentation. The peaks are symmetric, similarly to second-order TL peaks. As expected from the work by Chen and Pagonis (2008), the maximum intensity here is proportional to the value of n_0. Similar simulations have been performed with $A_m = A_n$ (not shown here). As expected, here, irrespective of the relation between $A_m m$ and $A_n(N-n)$, the second-order behavior is seen.

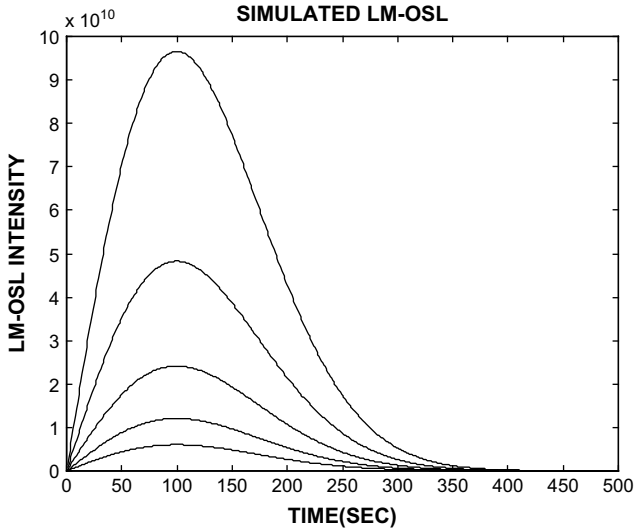

Fig. 2. LM-OSL simulated with $A_m = 10^{-5}$ cm^3 s^{-1}; $A_n = 10^{-10}$ cm^3 s^{-1}; $M = 10^{15}$ cm^{-3}; $N = 10^{14}$ cm^{-3}, $f_0 = 10^{-4}$ s^{-2}. The value of n_0 varies by factors of 2 in curves (a–e), being 10^{12} cm^{-3} in (a).

Fig. 6 shows the LM-OSL results of an intermediate case, the relevant parameters are given in the caption. Here, for the lowest value of n_0, $A_n(N-n)$ is about an order of magnitude larger than $A_m m$, whereas for the highest value, the former is smaller than the latter. The peak shifts here with the value of n_0, pointing to a non-first-order behavior. The ratio of L_{max} between the largest to smallest n_0 is here $\sim$48, which is rather superlinear, behaving like $\sim n_0^{1.4}$. Fig. 7 depicts the same results in the new presentation. Here, the dependence on n_0 is somewhat more than linear. The ratio between the maximum intensities is 18.38 for the change of n_0 by a factor of 16.

In the present work, we are dealing with single LM-OSL peaks, but in dosimetry and dating, it is common that a number of peaks occur. If there is some overlapping of components but peaks are

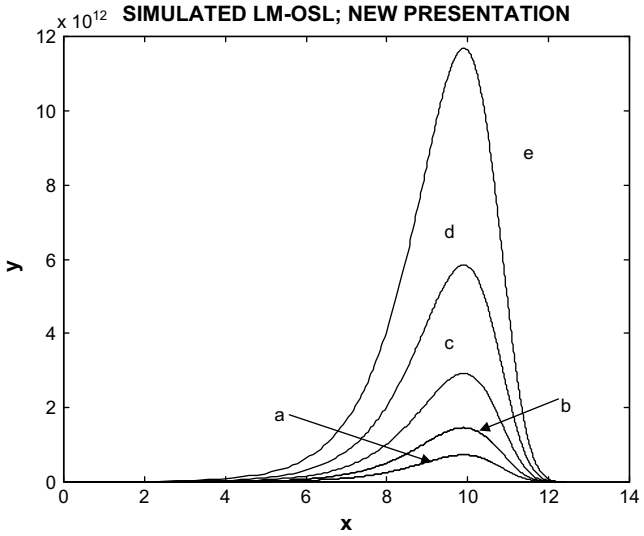

Fig. 3. The same results of Fig. 2, plotted in the new presentation. Here, $x = 2lnt$ and $y = t \cdot L(t)$.

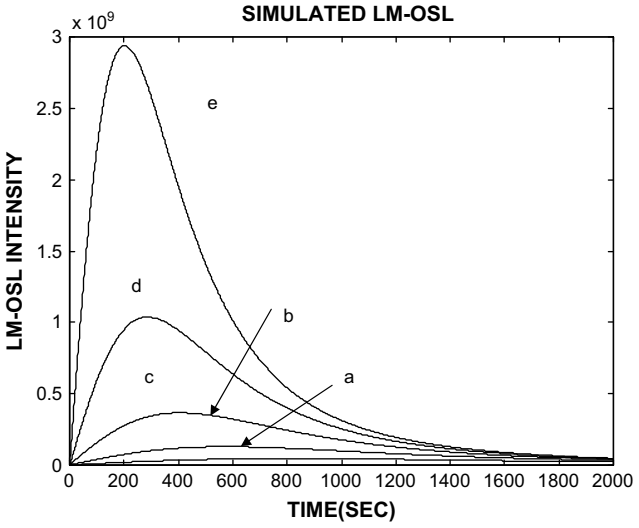

Fig. 4. LM-OSL simulated with $A_m = 10^{-12}$ cm^3 s^{-1}; $A_n = 10^{-11}$ cm^3 s^{-1}; $M = 10^{15}$ cm^{-3}; $N = 10^{14}$ cm^{-3}, $f_0 = 10^{-2}$ s^{-2}. The value of n_0 varies by factors of 2 in curves (a–e), being 10^{10} cm^{-3} in (a).

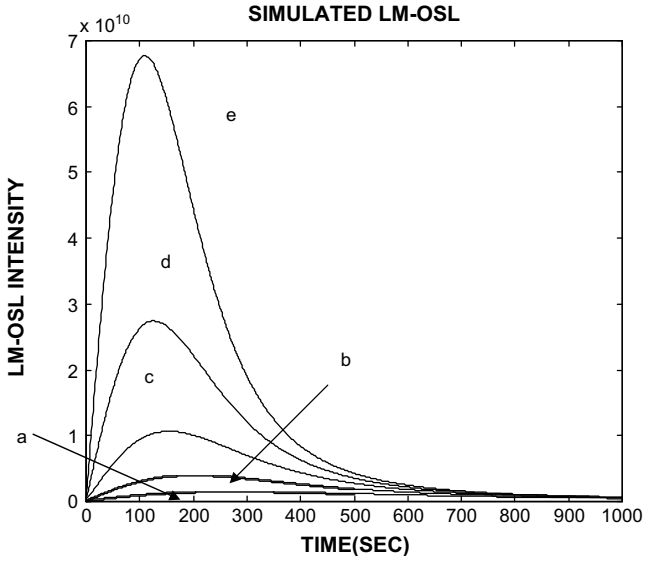

Fig. 6. LM-OSL simulated with $A_m = 10^{-9}$ cm^3 s^{-1}; $A_n = 10^{-10}$ cm^3 s^{-1}; $M = 10^{15}$ cm^{-3}; $N = 10^{14}$ cm^{-3}, $f_0 = 10^{-4}$ s^{-2}. The value of n_0 varies by factors of 2 in curves (a–e), being 10^{12} cm^{-3} in (a).

separated sufficiently, integration over certain interval may be used so as to maximize counts but at the same time to isolate as much as possible the different peaks. We have studied the behavior of such an area on n_0 in our simulations for the set of parameters used in Figs. 6 and 7, where the dependence on n_0 is strongly superlinear. We have taken the area under the curve from $t_m - \Delta t$ to $t_m + \Delta t$ where t_m is the time of maximum of the LM-OSL signal and Δt a selected time interval. For each value of Δt, the value of x in the approximate dependence ${n_0}^x$ has been determined. The results are shown in Table 1 and discussed below.

Let us consider the LM-OSL peak intensity in a more general way. For fixed initial concentration $\widehat{n_0}$ and fixed rate-constant ratio $\widehat{A}$, we can find, via Eq. (30), the value of concentration $\widehat{n}$ which maximizes the LM-OSL luminescence $\widehat{L}$. This was done using the numerical function maximizer fminbound from the package in SciPy (scientific Python). The value of the maximum luminescence $\widehat{L}$ can be plotted as shown in Fig. 8 as a function of n_0/N for different values of $\widehat{A}$. This log–log plot has a slope of 1.5 for large values of A_n/A_m, and is more than unity even for smaller values, which shows that the response of the LM-OSL maximum is superlinear except when kinetics are first-order; the response is linear only when $\widehat{n_0} \gg \widehat{A}$, i.e. $n_0 A_m \gg N A_n$.

The transformed LM-OSL can be studied similarly. We start by finding the values of $\widehat{n}$ which maximize Eq. (31) for fixed values of $\widehat{n_0}$ and $\widehat{A}$. This was done again with the same numerical maximizer. The values of $\widehat{t}\widehat{L}$ found from the maximizer are plotted against $\widehat{n_0}$ on a log–log scale in Fig. 9. Note that the peak of the transformed intensity, $\widehat{t}\widehat{L}$, depends on only two parameters, $\widehat{n_0}$ and $\widehat{A}$. Since Fig. 8 shows the peak plotted against $\widehat{n_0}$ for various values of $\widehat{A}$, this plot includes the entire parameter space. From Fig. 9, it is clear that the transformed LM-OSL peak intensity is mostly linear with n_0. Note that, unlike usual LM-OSL, the peak intensity of the transformed LM-OSL is independent of the experimental value of f_0, though its position depends on ${f_0}^{-0.5}$, as can be seen in Eq. (22).

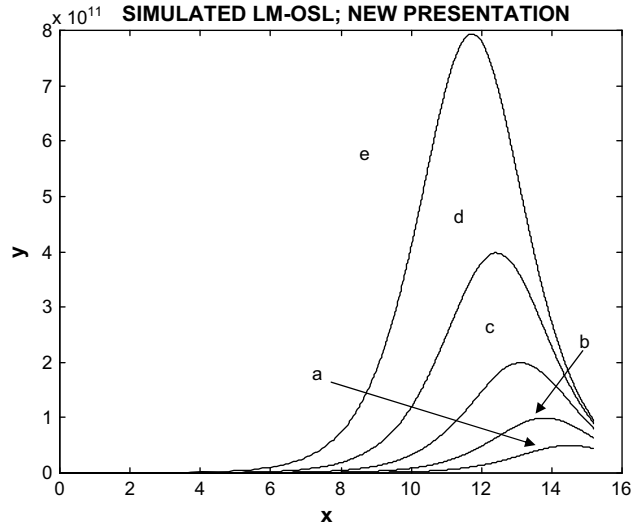

Fig. 5. The same results of Fig. 4, plotted in the new presentation; $x = 2lnt$ and $y = t \cdot L(t)$.

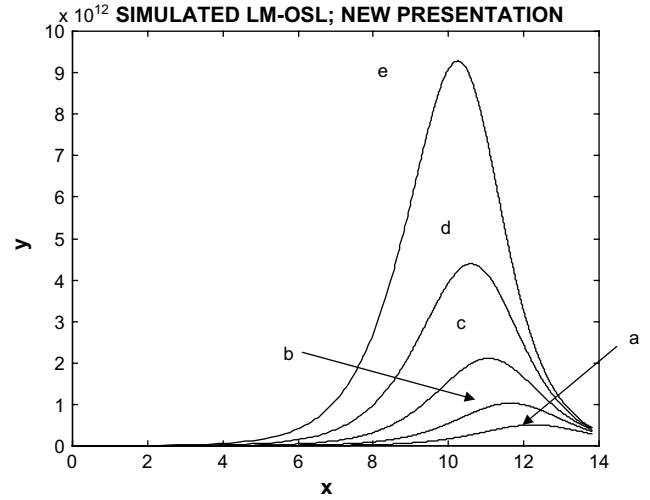

Fig. 7. The same results of Fig. 6, plotted in the new presentation; $x = 2lnt$ and $y = t \cdot L(t)$.

Table 1
Dependence of the power x of the dependence of the area under the LM-OSL peak on the time interval of integration. The parameters used for the simulations are the same as in Figs. 6 and 7. Integration was performed between $t_m - \Delta t$ and $t_m + \Delta t$.

Δt (s)	0	25	50	75	100
x	1.395	1.390	1.375	1.350	1.316

5. Discussion

In this work, we have studied the LM-OSL curves in their original and revised versions, by solving numerically the governing set of coupled differential equations, and by analytical means, using the one trap-one recombination-center model. By choosing sets of parameters leading to first-order kinetics, namely, dominating recombination, we have seen the characteristic behavior, i.e. that the LM-OSL peak maximum does not shift with the initial occupancy of traps. In addition, the shape of the new presentation resembled a first-order TL peak as expected and the maximum intensity depended linearly on n_0. The second-order case was seen either by having dominating retrapping or, alternatively, with the recombination and retrapping-probability coefficients being equal; in the former case, the trap has to be far from saturation. In both cases, the initial-concentration dependence of the original presentation was like $n_0^{1.5}$, and that of the revised one was linear, as expected. As for the intermediate cases, depending on the parameters chosen, intermediate dependencies on n_0 could be found. In the specific example shown in Figs. 6 and 7, in the original LM-OSL presentation, the initial-concentration dependence of the maximum could be given by $\sim n_0^{1.4}$. If we consider the dependence mentioned in Eq. (8), $L_{max} \propto n_0^{(b+1)/2}$, this yields an effective general order of $b = 1.8$. It should be noted, however, that this approach is entirely empirical, and had we evaluated the effective order from another feature of the curve such as its symmetry, we could have received a different value for b.

Regarding the n_0 dependence of the area under the LM-OSL curve mentioned above and summed up in Table 1, the maximum intensity depends superlinearly on n_0 with sets of parameters leading to second-order and intermediate cases whereas the total area from zero to infinity is always linear with n_0. One might expect that the integral over a fixed limited time interval will depend superlinearly on n_0, though a "weaker" superlinearity can be anticipated. Indeed, the value of x in the approximate power dependence is seen in Table 1 to be smaller when the interval of integration becomes larger. The value of x is still significantly larger than unity even when the integration goes from $t_m - 100$ to $t_m + 100$.

As for the new presentation of LM-OSL, with the same set of parameters, the dependence of the maximum intensity on the initial occupancy behaved like $\sim n_0^{1.05}$ in the example given, a very weak superlinearity as compared to the expected linearity for any value of b in the general-order presentation. The results of Fig. 9 show that the near-linear dependence of the transformed LM-OSL on n_0 takes place generally within the OTOR situation. However, one should not be surprised that there are slight deviations from linearity since one cannot expect the results of the simulation to fit exactly into the general-order framework.

It should be pointed out that the dependence of n_0 on the dose, which is very relevant to the dose dependence of the LM-OSL signal in its two presentations, has not been dealt with here. In cases where the trap occupancy is linear with the dose, the dependency of the LM-OSL maximum on the dose is, obviously, the same as that of n_0 discussed here. Other dependencies of n_0 can sometimes be expected, and will be discussed elsewhere. If, for example, $n_0(D)$ is a square-root function (Lawless et al., in press), this should be combined with the dependence of the LM-OSL signal on n_0. Thus, in

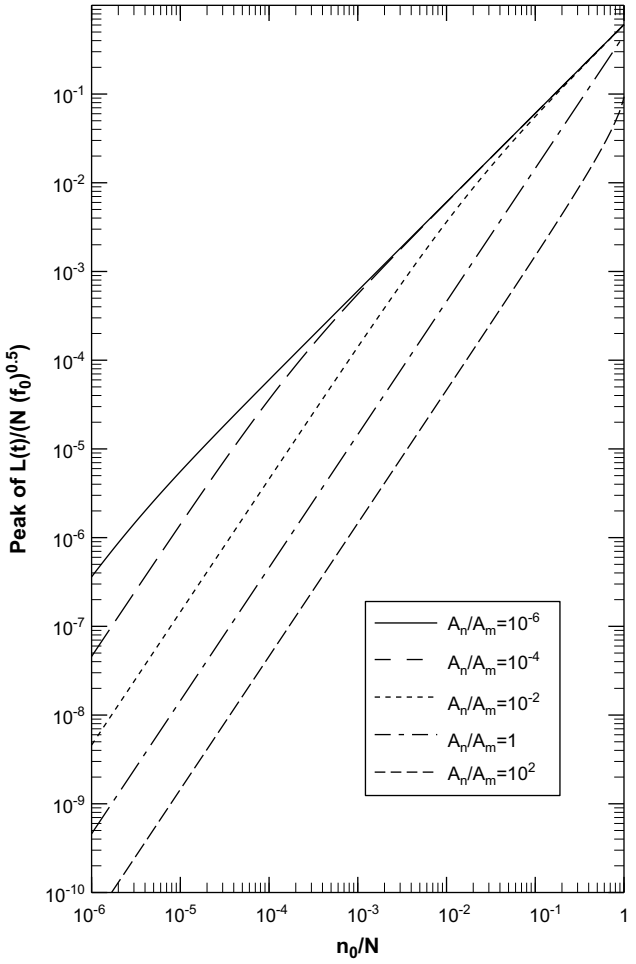

Fig. 8. The peak of luminescence as plotted against normalized initial concentration n_0/N for various values of $\tilde{A} = A_n/A_m$.

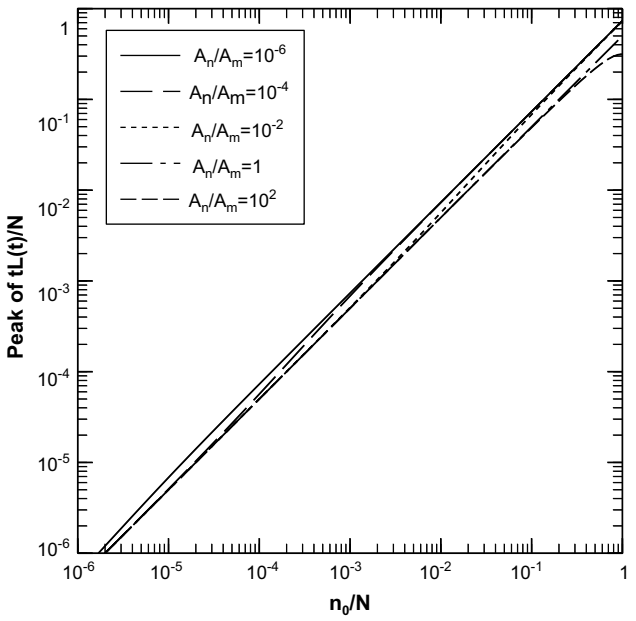

Fig. 9. The peak of the normalized transformed luminescence, tL/N, plotted against the normalized initial concentration, n_0/N for various values of $\tilde{A} = A_n/A_m$.

cases where the latter depends linearly on the dose, the signal will go like $D^{1/2}$, whereas if $n_0(D) \propto D^{3/2}$, the LM-OSL maximum may go like $D^{3/4}$. Obviously, the question of whether the LM-OSL maximum is linear with the excitation dose is of great importance for dosimetry and dating. Therefore, before using the procedure for dose evaluation, the dose dependence of the specific material under study should be established.

Acknowledgement

We would like to thank the anonymous referees for some important comments and suggestions which improved this work significantly.

References

Bulur, E., 1996. An alternative technique for optically stimulated luminescence. Radiat. Meas. 26, 701–709.

Bulur, E., Göksu, H.J., 1999. IR-stimulated luminescence from feldspars with linearly increasing excitation light intensity. Radiat. Meas. 30, 505–512.

Chen, R., Kristianpoller, N., 1986. Investigation of phosphorescence decay using TL-like presentation. Radiat. Prot. Dosimetry 17, 443–446.

Chen, R., McKeever, S.W.S., 1997. Theory of Thermoluminescence and Related Phenomena. World Scientific, Singapore.

Chen, R., Pagonis, V., 2008. A unified presentation of thermoluminescence (TL), phosphorescence and linear-modulated OSL (LM-OSL). J. Phys. D: Appl. Phys. 41 035102 (1–6).

Garlick, G.F.J., Gibson, A.F., 1948. The electron trap mechanism of luminescence in sulphide and silicate phosphors. Proc. Phys. Soc. 60, 574–590.

Halperin, A., Braner, A.A., 1960. Evaluation of thermal activation energies from glow curves. Physiol. Rev. 117, 408–415.

Huntley, D.J., Godfrey-Smith, D.I., Thewalt, M.L.W., 1985. Optical dating of sediments. Nature 313, 105–107.

Lawless, J.L., Chen, R., Pagonis, V. Sublinear dose dependence of thermoluminescence and optically stimulated luminescence prior to the approach to saturation level. In: Presented in LED 2008, 12th Int. Conf. Lumin. ESR Dating, Beijing, Sept. 2008. Radiat. Meas., in press.

Randall, J.T., Wilkins, M.H.F., 1945. Phosphorescence and electron traps. Proc. R. Soc. London A184, 365–407.

Rasheedy, M.S., 1993. On the general-order kinetics of thermoluminescence glow peak. J. Phys.: Condens. Matter 5, 633–636.

Visocekas, R., 1978. La luminescence de la calcite après irradiation cathodique: TL et luminescence par effet tunnel. Thèse, Université Pierre et Marie Curie, Paris 6.